



# A study on excitation of intrinsic localized modes in macro-mechanical cantilever array with tunable potentials

Masayuki Kimura<sup>†</sup> and Takashi Hikihara<sup>‡</sup>

<sup>†</sup>School of Engineering, The University of Shiga Prefecture  
 2500 Hassaka-cho, Hikone, Shiga 522-8533 Japan

<sup>‡</sup>Department of Electric Engineering, Kyoto University  
 Katsura, Nishikyo-ku, Kyoto 615-8510 Japan

Email: kimura.m@e.usp.ac.jp, hikihara@kuee.kyoto-u.ac.jp

**Abstract**—A mechanical cantilever array having non-linearity caused by magnetic forces has been produced for experimental study on intrinsic localized modes (ILMs). It was already reported that several ILMs were successfully observed and manipulated. This paper discusses the basic property of ILMs such as the coexistence and the stability. In addition, frequency response of ILM is numerically investigated for both two- and eight-degree-freedom systems.

## 1. Introduction

Since A. J. Sievers and S. Takeno discovered intrinsic localized mode (ILM) in an anharmonic lattice [1], the energy localized vibration has attracted many interests from researchers. In this decade, experimental studies have appeared [2], for example, in micro-cantilever arrays [3]. The experiments in micro-cantilever arrays [4] allow us to expect to realize applications of ILM in micro- or nano-engineering field.

For realization of such application, it is necessary to establish control scheme for ILM. Therefore, the dynamics should be understood not only for standing one but also for traveling one. We have numerically investigated ILMs in a mathematical model describing vibrations of micro-cantilever array. It was reported that coexisting ILMs show the stability change [5] and traveling ILM can be manipulated by the capture and release manipulation [6].

A macro-cantilever array, introduced in this paper, was newly proposed to confirm the numerical results experimentally [7], because constructions, adjustments, and measurements in macro-scale are easier than that in micro-/nano-scale. The cantilever array has an adjusting mechanism of nonlinearity of each cantilever. This feature allows to change the characteristics of the array dynamically. The attractive manipulation by inducing an impurity is realized by the individually adjustable nonlinearity [7].

In this paper, the macro-mechanical cantilever is briefly introduced and modeled at first. Then experimental observations are reported. In Sec. 3, stability of coexisting ILM is investigated. Finally, bifurcation diagrams are shown for two- and eight-degree-of-freedom systems.

## 2. Cantilever array

The schematic configuration of the macro-mechanical cantilever array is shown in Fig. 1(a). Eight elastic beams are arranged in one dimension and with a constant pitch. The upper end of each beam is fixed by the stiff support. Then each beam behaves as a cantilever. The elastic rod, called coupling rod, is attached near the support. Adjacent cantilevers are coupled each other. At the free end of each beam, the permanent magnet (PM) is attached. In addition, the electromagnet (EM) is placed to face PM. The whole of the cantilever array except EMs is vibrated by the voice coil motor.

The pair of magnets induces a nonlinear restoring force to each cantilever (see Fig. 1(b)). For simplicity, Coulomb's law for magnetic charges is applied to describe the nonlinearity with respect to the displacement of the tip of cantilever. By using small amplitude approximation, the magnetically induced force

$$F(u_n) = \frac{m_p m_e (I_{EM})}{4\pi\mu_0} \frac{u_n}{(u_n^2 + d_0^2)^{\frac{3}{2}}} = \chi(I_{EM}) \frac{u_n}{(u_n^2 + d_0^2)^{\frac{3}{2}}}, \quad (1)$$

is obtained [7], where  $m_p$  and  $m_e$  correspond to magnetic charges of PM and EM, respectively.  $d_0$  denotes the displacement between PM and EM when the cantilever is at rest. Since the magnitude of  $m_e(I_{EM})$  can be varied by the current flowing in EM, the nonlinearity is an adjustable parameter in the array.

To describe the motion of the array, only the first mode of cantilever is focused on for reducing the Euler-Bernoulli beam equation to an ordinary differential equation. As a

Table 1: Parameter symbols and their estimated values in Eq. (2), where  $\chi(I_{EM}) = \chi_0 + \chi_1 I_{EM}$ .

Symbol	Value	Symbol	Value
$\omega_0$	$2\pi \times 35.1$ rad/s	$\gamma$	$1.5$ s <sup>-1</sup>
$C$	$284$ s <sup>-2</sup>	$\chi_0$	$-4.71 \times 10^{-5}$ m <sup>3</sup> /s <sup>2</sup>
$d_0$	$3.0$ mm	$\chi_1$	$-9.14 \times 10^{-3}$ m <sup>3</sup> /s <sup>2</sup> A
$A$	$3.0$ m/s <sup>2</sup>	$\omega$	$2\pi \times 36.1$ rad/s

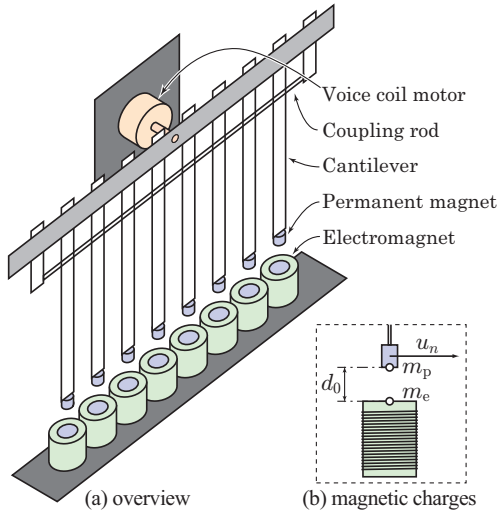


Figure 1: Configuration of (a) cantilever array and (b) magnetic charges.

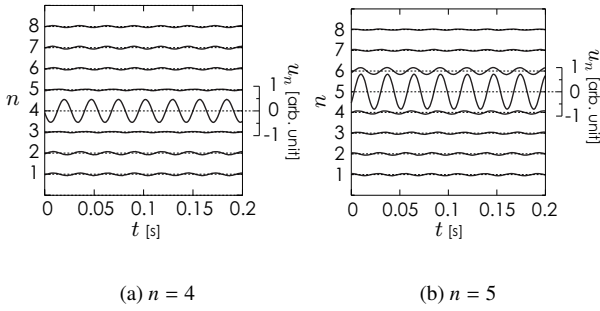


Figure 2: Experimentally observed ILMs.

result, the following equation is obtained [7],

$$\ddot{u}_n = -\omega_0^2 u_n - \gamma \dot{u}_n + F(u_n) + A \cos(\omega t) - C(u_n - u_{n+1}) - C(u_n - u_{n-1}), \quad (2)$$

where  $n = 1, 2, \dots, N$  for  $N$ -degree-of-freedom system. The second term,  $-\gamma \dot{u}_n$  is a damping term which is caused by air friction, *etc.* The external force is assumed to be sinusoidal function.  $C$  denotes the linear inter-site coefficient. In this paper, the boundaries of the array are set to be fixed, namely,  $u_0 = u_{N+1} = 0$ . The estimated values for Eq. (2) are listed in Table 1.

### 3. Coexisting ILMs and its stability

#### 3.1. Experimental excitation

Experimentally observed ILMs are shown in Fig. 2. Only one cantilever shows a large amplitude oscillation while the others are at almost rest. The energy of the array is clearly localized. At the same condition as Fig. 2, several ILMs were observed. In addition, the ground state that all the cantilever oscillate in small amplitude is realized. Numerical simulations confirm these observations [7]. Thus,

Eq. (2) is an appropriate model to study ILMs in the macro-mechanical cantilever array.

#### 3.2. Coexisting ILMs

The experimentally observed ILMs have only one site which shows large amplitude oscillation. These ILMs are classified into ‘‘Sievers-Takeno (ST) mode’’ [8]. On the other hand, ‘‘Page (P) mode’’ [8] is known as another kind of ILM that two neighboring sites excite [9]. P-modes could not be observed at the parameter listed in Table 1. It implies that P-modes are unstable. Numerical simulation is thus applied to discuss the coexistence and the stability of ILMs.

To obtain ILM solution, the anticontinuous limit is applied [10]. In the anticontinuous limit, an initial condition is freely chosen at the no-coupling regime. A localized solution is obviously obtained. After the coupling coefficient is slightly changed, the calculation to obtain periodic solution is applied again. If a similar localized solution to the initial condition is obtained, the coupling coefficient is changed. The above procedure is iterated until the coupling coefficient reaches to the desired value.

Each cantilever has tree state when it excited at 36.1 Hz. That is, stable resonance, unstable resonance, and stable ground state. Therefore, these states can be chosen as an initial condition for the anticontinuous limit. For localized solutions, only one or two cantilevers are set at the stable or the unstable resonance while the others are set at the stable ground state. The upper suffix of  $ST5^s$  implies that the 5th cantilever is set at the stable resonance at the initial step of the anticontinuous limit.  $P4^u-5^u$  is labeled in the same manner, namely, the 4th and 5th cantilevers are set at the unstable resonance.

Figure 3 show the wave form of coexisting ILMs obtained by the anticontinuous limit. For ST-modes, only one cantilever shows large amplitude oscillation. On the other hand, two neighboring cantilevers oscillate in phase. The difference between  $ST5^s$  and  $ST5^u$  ( $P4^s-5^s$  and  $P4^u-5^u$ ) is the phase of excited cantilever against the external force  $A \cos \omega t$ .

#### 3.3. Stability

To identify the stability of ILM, Floquet multipliers are obtained and shown in Fig. 4.  $ST5^s$  is stable in the sense of Lyapunov because all the multipliers are inside unit circle. On the other hand,  $ST5^u$  is unstable. One of the multipliers is outside unit circle. The stability of ST-mode seems to depend on the initial condition of the anticontinuous limit.

For P-mode,  $P4^s-5^s$  is unstable even though the initial condition is stable. In general, the stability depends on the spatial symmetry of ILM [8]. P-mode centered between sites usually unstable in discrete nonlinear Klein-Gordon lattices that nonlinear oscillators are linearly coupled. The macro-cantilever array is also a discrete nonlinear Klein-Gordon lattice. Therefore, P-modes is unstable.

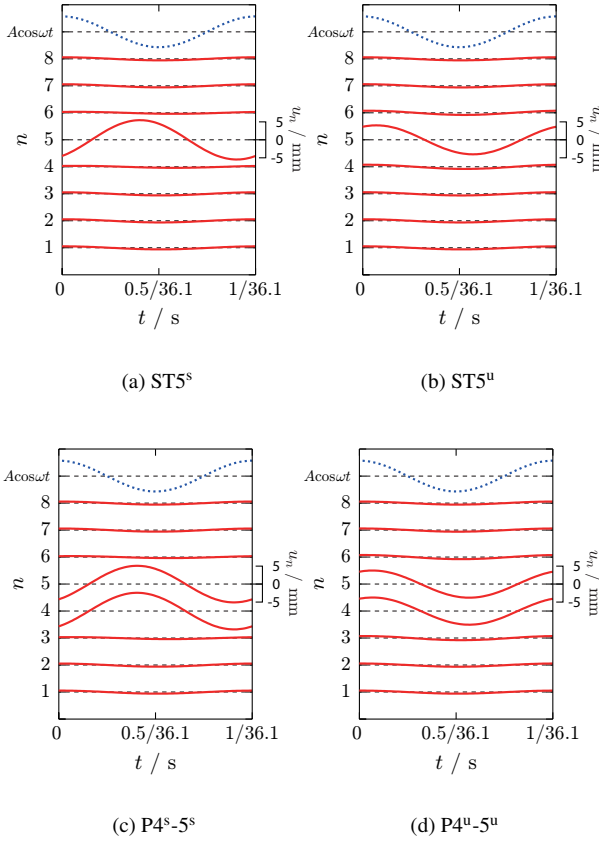


Figure 3: Numerically obtained ILMs by using the anticontinuous limit.  $P4^u-5^s$  ( $P4^s-5^u$ ) does not coexist for this case. It can survive if the coupling coefficient  $C$  is sufficiently small.

For  $P4^u-5^u$ , two Floquet multipliers are outside unit circle. It seems to be contributed by two things which are the symmetry and the initial condition.

## 4. Frequency response

### 4.1. Two-degree-of-freedom system

The amplitude of coexisting ILMs depends on the frequency of the external force. For simplicity, we start with the case of two-degree-of-freedom system. Fig. 5 shows the frequency response of the coexisting ILMs which has the same frequency as the external force. Two peaks are observed at  $f \approx 35.5$  Hz. The inset clearly shows that  $ST1^s$  and  $ST1^u$  disappear via a bifurcation as the frequency decreases. It is very similar to the case of one oscillator in which the stable resonance and the unstable resonance simultaneously disappear. For the P-modes, the situation is the same.

$ST1^u$  ( $ST2^u$ ) and  $P1^u-2^u$  appear from ZBM at  $f \approx 37.25$  Hz. This bifurcation is also similar to the case of one oscillator. Therefore, at the parameter listed in Table 1, the frequency response curve of individual oscillator is pre-

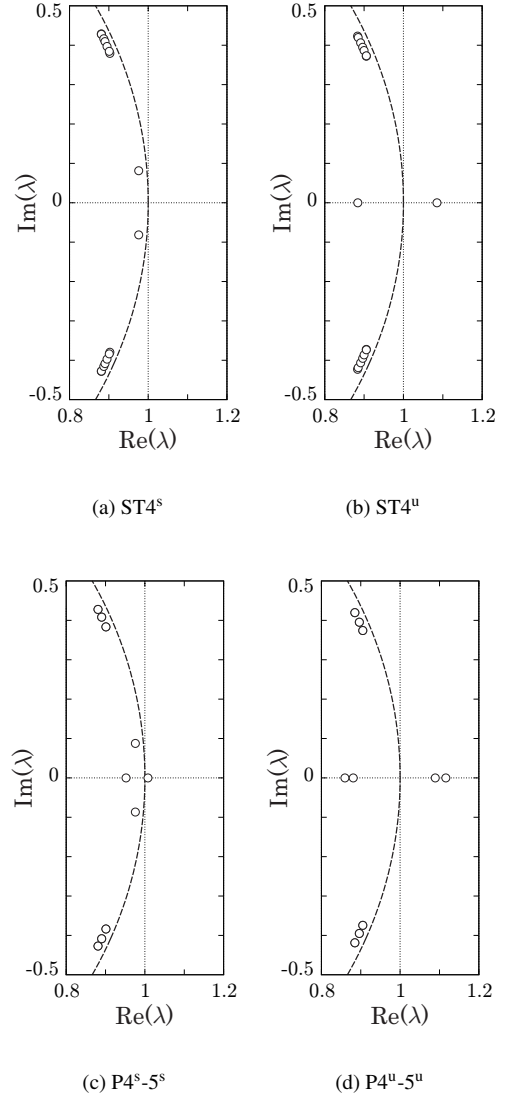


Figure 4: Floquet multipliers for ILMs shown in Fig. 3. The solid curve indicate unit circle on complex plane. All the multipliers are found around +1.

served.

### 4.2. Response of localized modes

The frequency response curve for ILMs shown in Fig. 3 is shown in Fig. 6. Because of the number of cantilevers, the frequency response curve become complicated. Then the other ILMs are not shown. The shape of curves are very similar to that in Fig. 5. It implies that the coupling coefficient is weak and the boundary of the array does not affect the response curve. However, ZBM in higher frequency region is not connected to  $P1^s-2^s$ . The fact suggests that many solution which is not localized concern the bifurcation between ZBM and ILMs in higher frequency region. On the other hand, in the lower frequency region, the bifurcation between ZBM and ILMs is similar to that of Fig. 5.

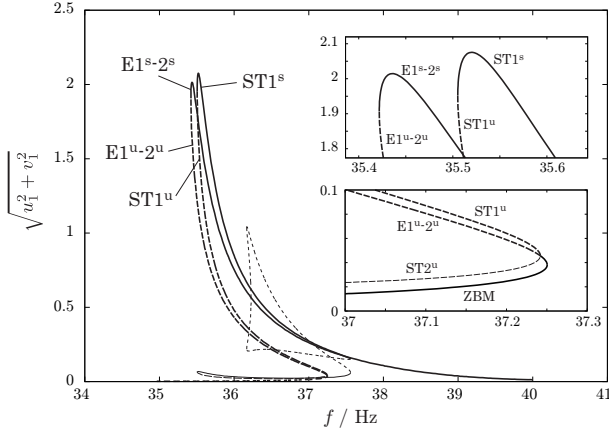


Figure 5: Frequency response curves of coexisting ILMs for two-degree-of-freedom system. ZBM indicates the ground state that all the cantilever oscillate with small amplitude. Insets shows enlargement near the bifurcation points.

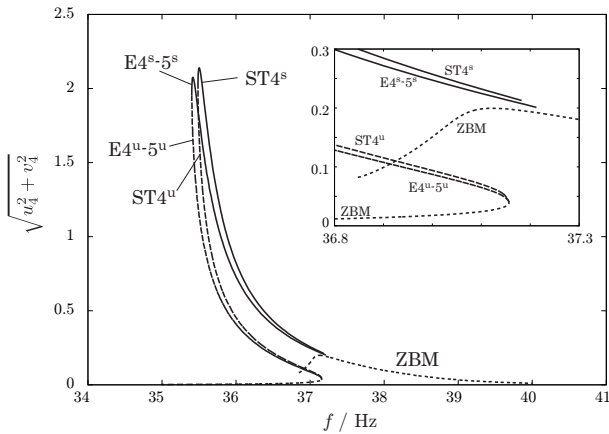


Figure 6: Frequency response curves of coexisting ILMs for eight-degree-of-freedom system. Only  $ST5^s$ ,  $ST5^u$ ,  $P4^s-5^s$ ,  $P4^u-5^u$ , and ZBM are shown.

## 5. Conclusion

In this paper, we briefly introduced the macro-mechanical cantilever array which equips the mechanism for tuning the nonlinearity of each cantilever. After the observation of ILM was shown, several kinds of ILM which coexist in the array were numerically investigated. As a result, the stability of ILM is affected by both the initial condition of the anticontinuous limit and the spatial symmetry of ILM. The frequency responses were shown for two- and eight-degree-of-freedom system. They show similar structure to each other. This implies that the produced cantilever array is under weak coupling regime. Therefore the characteristics of individual cantilever clearly remain.

## Acknowledgments

This work was supported by the Ministry of Education, Culture, Sports, Science and Technology in Japan, Grant-in-Aid for Young Scientist (B) No. 22760280.

## References

- [1] A. J. Sievers and S. Takeno, "Intrinsic localized modes in anharmonic crystals," *Phys. Rev. Lett.*, vol.61, p.970, 1988.
- [2] S. Flach and A. V. Gorbach, "Discrete breathers – advances in theory and applications," *Phys. Rep.*, vol.467, p.1–116, 2008.
- [3] M. Sato, B. E. Hubbard, A. J. Sievers, B. Ilic, D. A. Czaplewski, and H. G. Craighead, "Observation of locked intrinsic localized vibrational modes in a micromechanical oscillator array," *Phys. Rev. Lett.*, vol.90, p.044102, 2003.
- [4] M. Sato, B. E. Hubbard, and A. J. Sievers, "Colloquium: Nonlinear energy localization and its manipulation in micromechanical oscillator arrays," *Rev. Mod. Phys.*, vol.78, p.137, 2006.
- [5] M. Kimura and T. Hikihara, "Stability change of intrinsic localized mode in finite nonlinear coupled oscillators," *Phys. Lett. A*, vol.372, p.4592, 2008.
- [6] M. Kimura and T. Hikihara, "Capture and release of traveling intrinsic localized mode in coupled cantilever array," *Chaos*, vol.19, (1) p.013138, 2009.
- [7] M. Kimura and T. Hikihara, "Coupled cantilever array with tunable on-site nonlinearity and observation of localized oscillations," *Phys. Lett. A*, vol.373, (14) p.1257, 2009.
- [8] S. Flach and A. Gorbach, "Discrete breathers in Fermi-Pasta-Ulam lattices," *Chaos*, vol.15, p.15112, 2005.
- [9] J. B. Page, "Asymptotic solutions for localized vibrational modes in strongly anharmonic periodic systems," *Phys. Rev. B*, vol.41, p.7835, 1990.
- [10] L. M. Marín and S. Aubry, "Breathers in nonlinear lattices: numerical calculation from the anticontinuous limit," *Nonlinearity*, vol.9, p.1501, 1996.